Identification of a novel transasparaginase activity of *Bacillus Subtilis* (bTG) for sequence-specific bioconjugation.

Marie Flamme [†]*, Raphael Göhring [†], Denise Zamarbide [‡], Corentin Bon [‡], Alexandra Vissières [‡], Anne Basler [‡], Daniela Miranda [‡], Rainer Kneuer [‡], Greg Mann [†]*

[†] Chemical and Analytical Development, Novartis Pharma AG, 4056-CH Basel, Switzerland
[‡] Biomedical Research, Novartis Pharma AG, 4056-CH Basel, Switzerland

Bioconjugation, transglutaminase, biocatalysis, site-specific.

ABSTRACT: The ability of *bacillus subtilis* transglutaminase (bTG) to functionalize BSA has been investigated using peptide mapping experiments. Interestingly, the conjugation was not detected on a glutamine but on an asparagine residue. A sequence determination study was further performed and a sequence of ten amino acids for site specific conjugation was identified. A monobody showing no native reactivity with the bTG enzyme was produced with the identified peptide sequences and successfully conjugated to various types of substrates in very high yields (>90 %) with a 1/1/1.5 ratio of protein/amine/enzyme. Direct conjugation to the amino linker of a small interfering RNA (siRNA) was achieved in good yield and no impact on the siRNA activity was observed following the conjugation. The identified sequences were further engineered in VHH and IgG scaffolds and successful conjugation could also be observed with both small molecules and siRNA, confirming the potential of bTG for site-specific enzymatic bioconjugation.

INTRODUCTION

The functionalization of biopolymers with a variety of payloads is a common and well-established strategy to alter their properties, enabling numerous applications such as detection, drug delivery or the immobilization of biological compounds.[1,2] This technique is particularly used in the oligonucleotide field, as the conjugation of oligonucleotide with polyethylene glycol (PEG), cholesterol or proteins is an effective way to reduce the rapid kidney clearance of oligonucleotides and enhance their pharmacokinetics properties.[3,4] A common way to improve the delivery of antisense oligonucleotides (ASO) or small interfering RNA (siRNA) to their site of action is their bioconjugation to *N*-acetylgalactosamine (GalNAc), peptides (in case of cell targeting or cell penetration) or even antibodies.[5,6] Antibodies properties can themselves be improved by means of bioconjugation. The attachment of one or several drugs to create an

antibody drug conjugate (ADC) combines the target specificity of antibodies with the cytotoxic potency of the drug.[7] Despite the rapid expansion of bioconjugates, only a small number of new methods have emerged to improve the chemistry behind the modification of therapeutic proteins. Current methods are mainly based on the reactivity of maleimides and cysteines or N-hydroxysuccinimide esters and lysines.[8,9] Even if high conjugation yields can be obtained with these techniques, the abundance of cysteines and lysines in a protein sequence makes the number of payloads and the location of the conjugation difficult to control. The absence of regiospecificity in the conjugation reaction leads to a heterogeneous distribution of the payload, potentially resulting in a loss of activity, different therapeutic responses, and a lack of reproducibility. Due to their regio- and stereoselectivity under biologically compatible conditions, enzymes arise as powerful tools for bioconjugation applications.[10,11] Therefore, the development of a site specific bioconjugation tag, which would be orthogonal to well established approaches and act as a universal tag, would allow the conjugation at defined locations of any protein or peptide scaffold of choice.

In this context, transglutaminases are enzymes able to catalyze an acyl transfer reaction between the carboxamide group of glutamine (Q) and the amino group of a lysine residue in the presence of Ca^{2+}, resulting in the formation of an isopeptide bond and a release of ammonia.[12] Amongst this family of enzymes, bacterial transglutaminases have raised as attractive targets for bioconjugation, due to their broader substrate specificity, their calcium independency and their smaller molecular weight. *Streptomyces mobaraensis* transglutaminase (mTG) is one of the most used transglutaminase in the food industry and has been intensively studied, leading to a deep understanding of its mechanism of action.[13] It has been reported that site specific conjugation can be achieved with mTG, upon the insertion of the recognition sequence LLQG.[14] Strop *et al*. used this sequence to successfully conjugate various payloads to antibodies and investigated the effect of the conjugation site on the ADC stability and pharmacokinetics.[15] However, the heterologous expression of wild type mTG in *Escherichia Coli* (*E. Coli*) was shown to be challenging and only mutated enzymes produced in *E. Coli* were reported.[16,17]

As mTG paved the way for an enzymatic, site specific bioconjugation, another bacterial transglutaminase, the *bacillus subtilis* transglutaminase (bTG) has also been reported as a potential candidate for site specific conjugation. bTG was reported to recognize the sequence YAHQAHY, which could be inserted in a test protein and fluorescently labelled with dansylcadaverine.[18] The bioconjugation reaction is also not restricted to the natural lysine substrates as the bTG enzyme has been shown to tolerate other types of primary amines.[19] However, the recognition of the glutamine residue by a transglutaminase is more stringent and has been described as dependent on the accessibility of the Q amino acid, which should be located on a flexible region.[20] This enzyme possesses the advantages of being easily produced in *E. coli*, is active under mild, aqueous conditions and does not require any additional cofactors.[21] Attracted by these convenient features and by the apparent specificity of the bTG transglutaminase, we studied the requirements, biocatalytic potential and scope of this enzyme

and report here a different sequence specific site found under peptide mapping experiments for the conjugation of various primary amines (**Figure 1**).
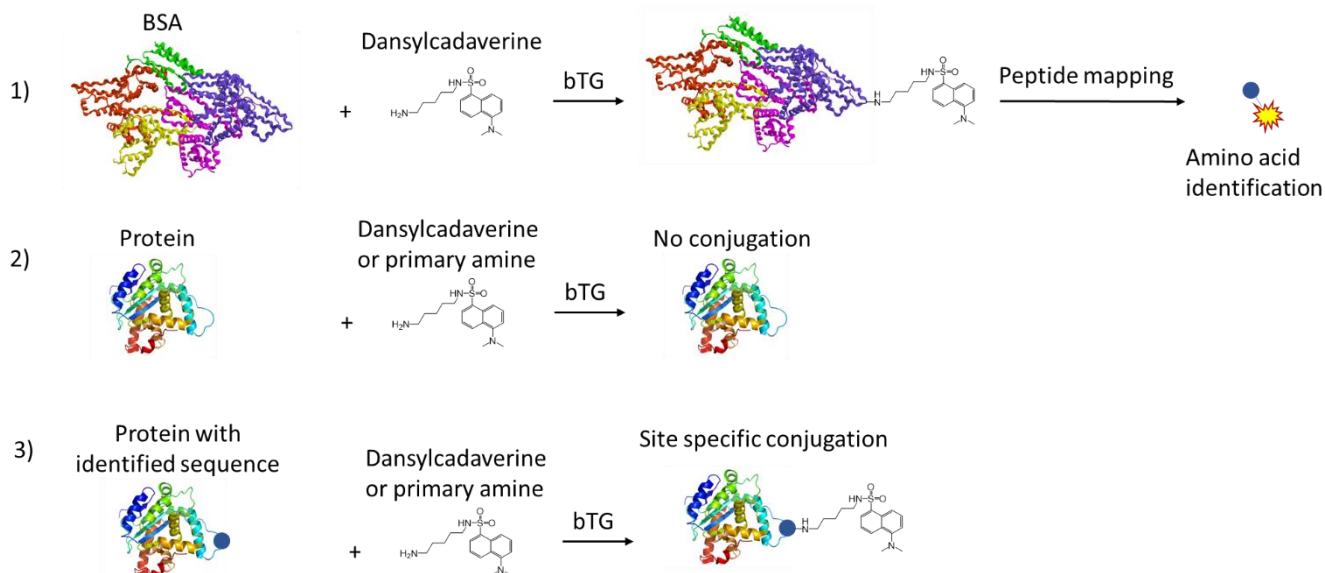

Figure 1. Aim of this work. In (1), peptide mapping experiments allow the identification of the amino acid bearing the dansylcadaverine moiety. After sequence determination, a protein showing no reactivity with the bTG enzyme (2) can be modified with the identified sequence and conjugated (3).

RESULTS AND DISCUSSION

In order to investigate the potential of the bTG transglutaminase to conjugate a primary amine in a sequence specific manner, we chose the monobody Mb(Lck_3) as a model target. This antibody mimetic is able to bind to the lymphocyte specific protein tyrosine kinase domain 2 (Lck-SH2 domain), an oncoprotein playing an important role in several cancers.[22–24]

The monobody was expressed in *E. coli* first with a C-terminal TEV-HIS tag (Mb(Lck_3)_CHis, **Figure S1** and **Table S1**). The bioconjugation reaction was tested with a dansylcadaverine as an amine donor, which enables easy detection at 335 nm and a home-made bTG purified enzyme (**Figure S2** and **Table S1**). The bioconjugation reaction led to no formation of the desired product (expected mass +318, **Figure S3** and **Table 1**). We then produced Mb(Lck_3)_CHis_bTG (**Figure S4** and **Table S1**), which includes the reported recognition sequence YAHQAHY between the monobody sequence and the TEV site. The bioconjugation reaction with this new sequence led to the desired product with an estimated 65% conversion (**Figure S5**, **Table S2** and **Table 1**). To confirm that the conjugation site was located on the glutamine of the reported recognition sequence, a Q100A mutant was prepared (**Figure S6** and **Table S1**), in which the glutamine was replaced by an alanine. Surprisingly, a conjugated product

could be detected and in higher yields compared to the model Mb(Lck_3)_CHis_bTG (**Figure S7**, **Table S2** and **Table 1**), indicating that the bioconjugation could be driven by other factors. The difference in reactivity between Mb(Lck_3)CHis and Mb(Lck_3)_Q100A could be due to the presence of the YAHAAHY linker, which could provide a change in the monobody structure and grant better accessibility to the reactive site.

Table 1. Summary of bioconjugation reactions performed on different Mb(Lck3) monobody systems with dansylcadaverine primary amine and bTG enzyme. Blue represents the monobody sequence, brown the TEV sequence, orange the His-Tag, red the reported recognition sequence for bTG enzyme, pink the inserted sequence and black a linker sequence.

Name	Sequence representation	Amine	Product (%)
Mb(Lck_3)_CHis	Monobody – ENLYFQGS – His-Tag	Dansylcadaverine (1eq)	0
Mb(Lck_3)_bTG_CHis	Monobody – YAHQAHY – ENLYFQGS – His-Tag	Dansylcadaverine (1eq)	65
Mb(Lck_3)_Q100A	Monobody – YAHAAHY – ENLYFQGS – His-Tag	Dansylcadaverine (1eq)	93
Mb(Lck_3)_NHis	His-Tag – ENLYFQ – Monobody	Dansylcadaverine (1eq)	57
Mb(Lck_3)_Q13A	His-Tag – ENLYFA – Monobody	Dansylcadaverine (1eq)	31
Mb(Lck_3)_N9A	His-Tag – EALYFQ – Monobody	Dansylcadaverine (1eq)	0
Mb(Lck_3)_N9A_Q13A	His-Tag – EALYFA – Monobody	Dansylcadaverine (1eq)	0
CS_BSA1	Monobody – LPETG – YICDNQDTISSK – His-Tag	Dansylcadaverine (1eq)	0
CS_BSA2	Monobody – LPETG – DAIPENLPPLTADFAEDK – His-Tag	Dansylcadaverine (1eq)	94
CS_Control1	Monobody – LPETG – HLVDEPQNLIK – His-Tag	Dansylcadaverine (1eq)	0
CS_Control2	Monobody – LPETG – TVMENFVQFVDK – His-Tag	Dansylcadaverine (1eq)	0
CS_1	Monobody – LPETG – DAIPENL – His-Tag	Dansylcadaverine (1eq)	93
CS_2	Monobody – LPETG – ENLPPLTADFAEDK – His-Tag	Dansylcadaverine (1eq)	83
CS_3	Monobody – LPETG – ENLPPL – His-Tag	Dansylcadaverine (1eq)	35
CS_4	Monobody – LPETG – ENL – His-Tag	Dansylcadaverine (1eq)	100
CS_5	Monobody – LPETG – DAIPENLPPL – His-Tag	Dansylcadaverine (1eq)	100
CS_6	Monobody – LPETG – GSGSENL – His-Tag	Dansylcadaverine (1eq)	88
CS_7	Monobody – LPETG – EQL – His-Tag	Dansylcadaverine (1eq)	0
CS_8	Monobody – LPETG – ANL – His-Tag	Dansylcadaverine (1eq)	36
CS_9	Monobody – LPETG – ENA – His-Tag	Dansylcadaverine (1eq)	89
CS_10	Monobody – LPETG – ANA – His-Tag	Dansylcadaverine (1eq)	29
CS_11	Monobody – LPETG – DNL – His-Tag	Dansylcadaverine (1eq)	49
CS_NC	DAIPENLPPL – LPETG – Monobody – LPETG – ENL – His-Tag	Dansylcadaverine (2eq)	98
CS_2C	Monobody – LPETG – DAIPENLPPL – AAAA – ENL – His-Tag	Dansylcadaverine (2eq)	92

This result led us to investigate other sequences to better understand the selectivity of the bTG enzyme and Mb(Lck_3)_NHis, possessing a His-Tag and a TEV site at the N-terminus (**Figure S8** and **Table S1**) was tested. Surprisingly, even in the absence of the recognition sequence, the conjugated product was formed at 57% (**Figure S9**, **Table S2** and **Table 1**). Replacement of the glutamine amino acid contained in the TEV site by an alanine (mutant Q13A, **Figure S10**

and **Table S1**) also led to conversion (**Figure S11**, **Table S2** and **Table 1**). As asparagine and glutamine share similar reactivity and structure, we also created the N9A mutant (**Figure S12** and **Table S1**) where the asparagine (N) was replaced by an alanine (A). With this sequence, no product formation could be observed (**Figure S13**, **Table S2** and **Table 1**) and the same result was found when both the asparagine and the glutamine were mutated by an alanine amino acid (N9A_Q13A, **Figures S14**, **S15**, **Tables S1**, **S2** and **Table 1**).

Intrigued by these findings, we decided to further investigate the bioconjugation site in a more rational manner. As bTG has been described to crosslink BSA[25], we reproduced and optimized the bioreaction between BSA and dansylcadaverine, catalyzed by the bTG enzyme (**Figure S16**). The reaction mixture was digested for peptide mapping experiments[26] and a control digestion was performed on BSA alone (**Figure S17**). The digested tryptic peptides were analyzed by mass spectrometry and the dansylcadaverine modification could be detected on two asparagine residues, N290 and N324. The extraction of the dansylcadaverine signature fragment confirmed the presence of the modification on these two amino acids. Surprisingly, no modification was detected on glutamine residues. By comparing the decrease in the intensity of the unmodified peptides containing N324 and N290 respectively, we propose the main conjugation site might be on N324 (**Figure S18**). Therefore, we ordered the two identified peptide sequences ("YICDNQDTISSK" and "DAIPENLPPLTADFAEDK", **Figures S19** and **S20**) and two control peptide sequences containing asparagine residues that are present in the BSA sequence but where no modification could be identified (**Figure S21** and **Figure S22**). Bioconjugation reactions with the dansylcadaverine amine were performed on the peptide sequences (**Figures S23** to **S26** and **Table S2**) where product formation could only be observed with the peptide sequence identified as the main binding site (N324, 96% conversion). Interestingly, this sequence possesses the same "ENL" motif as found in the TEV recognition sequence for which conversion could also be detected.

With these promising results, we expressed other Mb(Lck_3) mutants in order to identify the minimal sequence needed. As the bioreaction with an ENL-containing motif (TEV sequence) straight after the monobody sequence did not lead to any conversion (Mb(Lck_3)_CHis), whereas conversion could be observed when the recognition sequence was inserted in between (Mb(Lck_3)_bTG_CHis or Q100A mutant), we hypothesized that the structural accessibility of the conjugation site was an important factor. Therefore, we designed our new mutant sequences with a small, five amino-acid linker (LPETG) between the monobody sequence, which was available from previous investigations (data not shown) and the insert sequence. We then produced four mutants with the peptide sequences previously tested (CS_BSA1, CS_BSA2, CS_Control1, CS_Control2, **Figures S27** to **S30** and **Table S1**). Bioconjugation reactions followed the same trend as for the peptide sequences alone, with conjugated product formed only in the presence of the ENL-containing sequence (DAIPENLPPLTADFAEDK) and similar conversion (94% conversion, **Figures S31** to **S34**, **Table S2** and **Table 1**).

In order to better understand which amino acids are crucial for the bioconjugation mediated by the bTG enzyme, we produced eleven other mutants based on the CS_BSA2 identified conjugation sequence (CS_1 to CS_11, **Figures S35** to **S45** and **Table S1**) and tested them for conjugation with the dansylcadaverine moiety (**Figures S46** to **S56**, **Table S2** and **Table 1**). Shortening the sequence to DAIPENL (CS_1) had no impact on the percentage of conversion. The four amino acids DAIP do not appear as essential for the recognition as a similar conjugation could be obtained with a random GSGS sequence (CS_6). The addition of three amino acids between the ENL-reactive site and the His-Tag led to full conversion (CS_5). On the other hand, when the size of the linker sequence between the reactive site and the monobody sequence was shortened, a diminution in conversion was observed (CS_2 and CS_3). Surprisingly, when the sequence was reduced to the "ENL" pattern, 100% conjugated product was obtained (CS_4). As a control, we also tested the "EQL" sequence, for which no conversion could be detected, therefore confirming the specific recognition of the asparagine over a glutamine (CS_7). Replacement of the glutamic acid (E) by an alanine led to a significant drop in conversion (CS_8) while its replacement by an aspartic acid (D) sharing similar reactivity and structure maintained moderate conversion (CS_11), albeit reduced compared with CS_4. The mutation of the leucine amino acid (L) by an alanine had less impact on the bioconjugation reaction (CS_9) whereas the mutation of both E and L by alanine had a deleterious effect on the formation of the conjugated product (CS_10). Taken together, these data suggest that while "ENL" might be sufficient to promote bioconjugation, local secondary or even secondary structural elements also play a role.

With two sequences providing 100% conversion, we designed monobody CS_NC which contains "DAIPENLPPL" at the N-terminus and the "ENL" moiety at the C-terminus (**Figure S57** and **Table S1**). The bioconjugation reaction with 2 equivalents of dansylcadaverine amine led to 98% conversion to the double conjugated product. No starting material could be identified; the remaining 2% corresponding with the single conjugated product (**Figure S58**, **Tables S2** and **Table 1**). A similar behavior was obtained with the monobody CS_2C which contains at the C-terminus the reactive sequence "DAIPENLPPL", a linker composed of four "A" amino acids and the "ENL" sequence. With two equivalents of amine, 93% conversion towards the double conjugated product was obtained (**Figures S59**, **S60**, **Tables S1**, **S2** and **1**). For both sequences, an excess of the amine reagent did not lead to a higher number of conjugated products (data not shown), confirming the specificity of the conjugation.

We next investigated the tolerance of the bTG enzyme towards amino substrates by screening various types of amine reagents. We first confirmed that the bTG was not able to accept secondary amines as substrates as no product formation could be observed with a panel of secondary amines (data not shown). We therefore studied the effect of the length of the linker and performed conjugation reactions between CS_BSA2 sequence and dansyl-based molecules containing a 4-carbon linker (molecule A, **Figure S61** and **Figure 2**), a 3-carbon linker

(molecule B, **Figure S62** and **Figure 2**) or a 2-carbon linker (molecule C, **Figure S63** and **Figure 2**). A decline in conversion was detected as the length of the linker was decreasing (100% for A, 81% for B and 31% for C, **Tables 2** and **S2**). As the natural substrate of bTG is the amino group of a lysine, we also tested a lysine molecule (D, **Figure S64** and **Figure 2**) and a lysine analogue (E, **Figure S65** and **Figure 2**) for conjugation and 100% conversion was observed for both molecules (**Tables 2** and **S2**). We then investigated smaller water-soluble molecules with a 1-carbon linker (F and G, **Figures S66, S67** and **Figure 2**) which led to 77% and 100% conversion respectively. Lastly, we also wondered if the bTG would be able to tolerate more bulky and complex molecules. Molecule H (**Figure S68** and **Figure 2**) which has been reported as a BRD inhibitor, gave full conversion (**Tables 2** and **S2**).[27] 91% conversion was obtained for molecule I (**Figures 2** and **S69**, **Tables 2** and **S2**) which acts as a kinase inhibitor.[28] Another important class of substrate are PEG chains, as they are commonly employed as linkers to attach a biologically relevant drug to an antibody. The presence of the PEG linker enables a decrease in immunogenicity, a better solubility, and a slower clearance of the antibody drug conjugate from the body.[29] In this regard, a PEG amine (molecule J, **Figure S70** and **Figure 2**) was tested and was fully tolerated by the bTG enzyme as 100% conversion was observed (**Tables 2** and **S2**). Lastly, siRNA-based therapeutics have emerged as a promising drug modality as these synthetic, double stranded RNA molecules are able to degrade a target mRNA in a sequence specific manner.[30] Despite their unlimited potential, their application in clinical settings is still restricted, due to the absence of effective delivery systems. Even though various conjugations of siRNA have already been reported, the current methods either lack specificity, with drug to protein ratios difficult to control, or are based on a specific type of chemistry, which requires careful design and preparation of the siRNA and protein moieties.[31–33] To the best of our knowledge, no direct enzymatic conjugation of siRNA to protein scaffolds has been reported to date. In our experiments, we tested molecule K, a siRNA that regulates the expression of AHSA1, a chaperone of heat shock 90 kDa (HSP90), which enhances the ATPase activity of the latter. AHSA1 plays a crucial role in cellular processes related to protein folding and stability and has been found to be overexpressed in numerous cancer cells.[34] This siRNA is composed of an antisense of 21 nucleotides and a sense strand (19-mer) containing a hexylamino tri acetamide amine at its 3'-end (**Figure 2**). We decided to test the bioconjugation with the two most promising sequences CS_4 and CS_5. We first performed conjugations tests (data not shown) and the best performing conditions were found with 3 equivalents of siRNA. The conversion was difficult to follow by LCMS as the peaks corresponding to the bTG, siRNA and parent monobody coeluted. We decided to proceed to the purification of the two reaction mixtures and CS_4_K conjugate was isolated with 56% yield and 93% purity and conjugated product CS_5_K was obtained with 76% yield and 99% purity (**Figures S73** and **S74**, **Tables 2** and **S2**). To confirm that the covalent coupling between the monobodies and the siRNA will not alter their gene silencing potency, lipofection of the siRNA conjugate was performed in HEPA1-6 cells (**Figure S75**). The results indicate a silencing efficiency of 87% for both CS_4_K and CS_5_K compounds at 100 nM, which relates similarly to the positive control (siRNA only), showing that the siRNA properties were not affected by the bTG bioconjugation.

7

This primary amine screening therefore confirms the broad scope of the bTG enzyme towards primary amino substrates. These results suggest that a variety of payloads can be attached by the bTG, including dyes, drugs, siRNA, and cell penetrating peptides that could further be used as carriers to deliver the monobody into cells.[35]
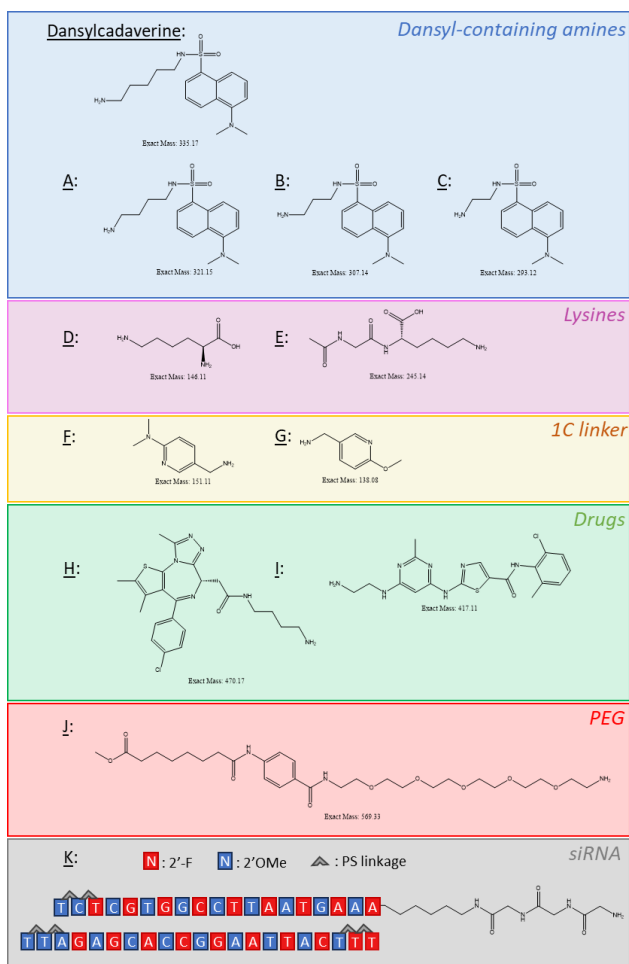

Figure 2. Structures of primary amines tested for bioconjugation reactions.

Table 2. Summary of bioconjugation reactions performed on different monobody systems with various primary amines and bTG. Blue represents the monobody sequence, orange the His-Tag, pink the inserted sequence and black a linker sequence.

Name	Sequence representation	Amine	Product (%)
CS_BSA2_A	Monobody > LPETG > DAIPENLPPLTADFAEDK > His-Tag >	A: dansyl, 4C linker	100
CS_BSA2_B	Monobody > LPETG > DAIPENLPPLTADFAEDK > His-Tag >	B: dansyl, 3C linker	81
CS_BSA2_C	Monobody > LPETG > DAIPENLPPLTADFAEDK > His-Tag >	C: dansyl, 2C linker	31
CS_BSA2_D	Monobody > LPETG > DAIPENLPPLTADFAEDK > His-Tag >	D: lysine	100
CS_BSA2_E	Monobody > LPETG > DAIPENLPPLTADFAEDK > His-Tag >	E: lysine analogue	100
CS_BSA2_F	Monobody > LPETG > DAIPENLPPLTADFAEDK > His-Tag >	F: 1C linker	77
CS_BSA2_G	Monobody > LPETG > DAIPENLPPLTADFAEDK > His-Tag >	G: 1C linker	100
CS_BSA2_H	Monobody > LPETG > DAIPENLPPLTADFAEDK > His-Tag >	H: BRD inhibitor	100
CS_BSA2_I	Monobody > LPETG > DAIPENLPPLTADFAEDK > His-Tag >	I: kinase inhibitor	91
CS_BSA2_J	Monobody > LPETG > DAIPENLPPLTADFAEDK > His-Tag >	J: PEG	100
CS_4_K	Monobody > LPETG > ENL > His-Tag >	K: siRNA	56 (final yield)
CS_5_K	Monobody > LPETG > DAIPENLPPL > His-Tag >	K: siRNA	76 (final yield)

Based on these results we decided to evaluate this sequence for conjugation on other proteins. First, we tested VHH single domain antibodies. VHH antibodies consists in the single variable domain of heavy chain antibodies. It possesses the high affinity and specificity of antibodies and its smaller size grants access to high stability and solubility as well as lower production costs, making them interesting candidates for clinical therapeutics, immunodiagnostics and environmental monitoring.[36,37] We took as a model a VHH antibody against epidermal growth factor receptor (EGFR), a protein involved in cell proliferation, differentiation, division and survival. EGFR is a well-established oncogenic driver that features high-level expression across multiple cancer indications of interest. EGFR inhibitors could slow down and regulate the EGFR signaling cascade.[38]

We first designed seven anti-EGFR VHH constructs: anti-EGFR_VHH consists in the VHH parent sequence as a negative control, anti-EGFR_VHH_ENL possesses the "ENL" conjugating sequence at the C-terminus without linker, anti-EGFR_VHH_ENL_H6 was designed with the "ENL" sequence followed by a His-Tag at the C-terminus, anti-EGFR_VHH_(G4S)3_ENL possesses a flexible linker between the VHH sequence and the conjugation sequence, anti-EGFR_VHH_(AP)4_ENL has a rigid linker between the VHH and the ENL sequences, anti-EGFR_VHH_LPETG_ENL bears the linker previously used in the monobody experiments and anti-EGFR_VHH_DAIPENLPPL is constructed with the longer conjugating sequence right after the VHH sequence. All proteins were successfully produced and analyzed by LCMS (**Figures S76** to **S82** and **Table S1**). We then performed the conjugation reactions using one equivalent of dansylcadaverine on all systems (**Figures S83** to **S89**, **Table S2** and **Table 3**). No conversion was achieved on the negative control composed of the VHH sequence alone, nor on any of the sequences ending by the conjugation tag "ENL". However, 94% conversion was obtained when a His-Tag was placed after the conjugation site and 84% conversion for the longer sequence "DAIPENLPPL". As previous conversion was achieved using the LPETG linker, we believe that

9

the bTG enzyme needs the presence of a few amino acids after the "ENL" conjugation site to be able to perform the conjugation.

Table 3. Summary of bioconjugation reactions performed on different VHH systems with dansylcadaverine or siRNA and bTG. Green represents the VHH sequence, orange the His-Tag, pink the inserted sequence and black a linker sequence.

Name	Sequence representation	Amine	Product (%)
Anti-EGFR_VHH	VHH	Dansylcadaverine (1eq)	0
Anti-EGFR_VHH_ENL	VHH ENL	Dansylcadaverine (1eq)	0
Anti-EGFR _VHH_ENL_H6	VHH ENL His-Tag	Dansylcadaverine (1eq)	94
Anti-EGFR _VHH_(G4S)3_ENL	VHH GGGGSGGGGSGGGGS ENL	Dansylcadaverine (1eq)	0
Anti-EGFR _VHH_(AP)4_ENL	VHH APAPAPAP ENL	Dansylcadaverine (1eq)	0
Anti-EGFR _VHH_LPETG_ENL	VHH LPETG ENL	Dansylcadaverine (1eq)	0
Anti-EGFR _VHH_DAIPENLPPL	VHH DAIPENLPPL	Dansylcadaverine (1eq)	84
Anti-EGFR _VHH_ENL_H6	VHH ENL His-Tag	siRNA K (1 eq)	>50%
Anti-EGFR _VHH_DAIPENLPPL	VHH DAIPENLPPL	siRNA K (1 eq)	>50%

The ability of bTG to conjugate one equivalent of siRNA (molecule K) to the VHH_DAIPENLPPL and VHH_ENL_H6 proteins was then investigated. Both LC analysis revealed a significant drop of the peaks corresponding to the parent proteins and the appearance of the conjugated peaks with a minimum of 50% conversion (**Figures S90** and **S91**, **Table 3**), confirming the broad tolerance of bTG towards primary amines.

The successful conjugation of VHH with small molecules and siRNA led us to challenge even further the bTG, by designing an immunoglobulin G (IgG) containing the "DAIPENLPPL" sequence either at the end of the light chain or at the end of the heavy chain (**Table S1**). The chosen antibody is targeting the transferrin receptor, which is responsible for the cellular iron uptake and is overexpressed in several types of cancer.[39] We tested the conjugation of dansylcadaverine on the unmodified parent IgG_LALA and on the antibody modified on both light chains (IgG_LALA_LC_DAIPENLPPL) or heavy chains (IgG_LALA_HC_DAIPENLPPL). In order to perform a better LCMS analysis of the reaction mixture, the reactions were reduced using urea, ammonium bicarbonate and dithiothreitol (DTT) in order to break the sulfur bridges between the chains, followed by a deglycosylation step using PNGaseF, to prevent the difference of retention time between different isoforms. This treatment resulted in a separation of the light and heavy chains by LCMS (**Figures S92** to **S94**). Conjugation with dansylcadaverine could be detected on both light chains of the IgG_LALA_LC_DAIPENLPPL with a 12% conversion and a drug to antibody ratio of 2 (**Figure S96** and **Table S2**). No

conversion could be detected with the negative control IgG_LALA nor on the antibody modified at the end of the heavy chain (**Figures S95** and **S97**). It is possible that the recognition sequence is more sterically hindered at the C-terminus of the IgG heavy chain than on a VHH domain, which precludes bioconjugation. Structural insight could help to better understand the requirements for activity by bTG. Conjugation of the light chain with siRNA was also achieved in longer reaction time (96 hours) and 10% conversion could be achieved (**Figure S98**).

CONCLUSION

To conclude, the ability of bTG enzyme to crosslink BSA was confirmed and peptide mapping experiments were carried out to determine the ligation site. Surprisingly, the identified site for the conjugation was found on an asparagine residue instead of the expected glutamine residue and did not match the recognition sequence reported in the literature. The insertion of this sequence on a non-reactive monobody sequence led to the conjugation of dansylcadaverine and other various primary amines in very good yields (>90%). Increasing the number of amine equivalents did not lead to a higher number of conjugates (data not shown), confirming that the bioconjugation reaction depends on the protein sequence. A deep investigation of the amino acids that are essential for the bioconjugation was performed and the recognition sequence could be reduced to the three amino acids "ENL" and the ten amino acids "DAIPENLPPL" sequences. However, the sequence itself is not the only requirement for the bioconjugation to be possible as it also depends on the accessibility of the reactive amino acids. Therefore, the insertion of the recognition sequence into a protein should be made with careful inspection of the structure of the protein of interest or with the addition of a longer sequence. Several small molecules could be attached to a monobody containing the sequence of interest in good yields, including an siRNA molecule. Conjugation of a small molecule and siRNA on different VHH could also be achieved and brought a better understanding of the sequence requirements, as a few amino acids are needed after the reaction "ENL" for a successful conjugation. A reduced conversion was achieved when IgG was used as a substrate, and a DAR 2 could be obtained on the light chains of the antibody, both with dansylcadaverine and siRNA. These results appear as a promising proof of concept for the more complex conjugation of antibodies and a good starting point for further enzyme evolution. The engineering of the antibody constant domain with an accessible conjugation site is also under consideration.

EXPERIMENTAL PROCEDURES

All reagents were purchased at reagent grade from different commercial suppliers and used without further purification unless otherwise described. Oligonucleotide primers were purchased from Microsynth or IDT and used without further purification. Peptides were purchased from LifeTein and used without further purification. All enzymes were prepared as described below. siRNA molecule K was aquired from AxoLabs GmbH and used without further purification.

11

General protocol used for protein expression and purification

All enzymes were synthesized and cloned into pCK900 vector and transformed into W3110 E. coli electro-competent cell by electroporation and plated on LB agar with 30 µg mL^{-1} chloramphenicol. A single bacterial colony was picked and grown in LB media (Teknova) supplemented with 1 % glucose and 30 µg.mL^{-1} chloramphenicol at 37°C, 200 rpm, 85 % humidity overnight. Following overnight growth, the culture was used to inoculate a shake flask containing TB media (Teknova) supplemented with 30 µg.mL^{-1} chloramphenicol and grown at 30°C, 200 rpm, 85 % humidity until the optical density (OD600) of the culture reached 0.7. Enzyme expression was induced by the addition of IPTG to a final concentration of 1 mM and the cultures further grown at 30°C, 200 rpm, 85 % humidity for 16 h. Cells were harvested by centrifugation at 4000 *g* at 4°C for 15 min and the media discarded. Cell pellets were frozen at − 80°C prior to lysis.

Cells were re-suspended in lysis buffer (50 mM Trizma® base pH 8.0, 150 mM NaCl, 20 mM imidazole, 1 mM DTT) and lysed via passage through a microfluidizer (Microfluidics, LM20). Lysate was clarified via centrifugation at 40 000 *g* at 4°C for 30 min and the supernatant was loaded on a pre-packed Ni-IDA column (Macherey-Nagel) pre-equilibrated in lysis buffer. The protein bound to the column was washed with 40 column volumes of lysis buffer and eluted in 2 column volumes of elution buffer (50 mM Trizma® base pH 8.0, 150 mM NaCl, 250 mM imidazole, 1 mM DTT). The purified protein was dialyzed into storage buffer (50 mM Trizma® base pH 8.0, 150 mM NaCl, 1 mM DTT, 10 % glycerol) and frozen at − 80°C.

General protocol for bioconjugation using bTG enzyme with small molecules amines.

Reactions were set up in a final volume of 50 µL. The target protein was used at a final concentration of 50 µM (1 eq), the amine donor at a final concentration of 50 µM (1eq) in a buffer containing 50 mM Trizma® base and 4.5 mM DTT at pH 8.0. The bTG enzyme was added last at a final concentration of 75 µM (1.5 eq). Reactions were shaken at 500 rpm and 37°C overnight and analyzed by LCMS experiments. Conversion is defined as the ratio of the product peak area over the sum of the area of the product and starting material multiplied by 100.

For IgGs, 20 µL of Urea 8M and 0.4 M NH_4HCO_3 and 2 µL DTT 1M were added to the reaction mixtures and samples were incubated at 50°C for 30 minutes. Then, 1 µL of PNGaseF (0.5 µg/µL) was added and the mixture was further incubated at 37°C for 3 hours.

General protocol for bioconjugation using bTG enzyme and siRNA amine

Reactions were set up on a 750 µg scale for monobodies and a 100 µg scale for VHH and IgGs. 1 equivalent of the target protein was used and 1-3 equivalents of siRNA in a buffer containing 50 mM Trizma® base at pH 8.0. The bTG enzyme was added last at 1.5 equivalents. Reactions were stirred at 500 rpm and 37°C overnight. For monobody and VHH conjugation, reaction

mixtures were analyzed using anSEC (Superdex 75 5/150 Increase, buffer PBS and a 0.3 mL/min isocratic elution). Purification of the monobodies were performed on an ÄKTA pure system with Superdex75 or HiLoad Superdex75 columns for monobody, the final conjugate was analyzed by SEC-MS. For IgG conjugation, reaction mixtures were analyzed using anIEX (Propac SAX 10 column, Buffer A: 10 mM Tris buffer, 20% EtOH pH 8, Buffer B: 10 mM Tris buffer, 20% EtOH + 1.5M NaCl pH 8. Gradient: 3 min at 10% B, 14 min to 100% B, 4 min at 100% B, 1 min to 10% B, 8 min at 10%B at a 0.75 mL/min flow rate)

LCMS analysis 10 min method

LCMS analysis was carried out on a Waters Acquity UPLC system and a 10 min method with 5% to 60% B in 8.0 min. Mass spectra over a mass range from 120 m/z to 3000 m/z are acquired using positive-ion Electrospray Ionization (ESI). Deconvolution range from 10 – 150 kDa using Maximum Entropy (MaxEnt).

Column: Acquity UPLC BEH C4, 2.1 x 100mm Column, 1.7 µm
Column Temperature: 80°C
Eluents: A: water + 0.05% TFA; B: isopropanol + 0.05% TFA
Gradient: initial 5% B; from 5 % to 60 % B in 8.0 min; from 60 % B to 98 % B in 0.2 min; hold 1.1 min 98 % B
Flow rate: 0.5 mL/min
Injection Mode: Partial loop
MS Method: Time: 0 – 9.8 min

Mass Range: 120 – 3000 m/z
Ionization mode: ES+

Data: Continuum

Scan Time: 1 sec
QTof Tune Page: Source:

Capillary: 3.00 kV

Sampling Cone: 120 V

Source Offset: 30

Temperatures:

Source: 130 °C

Desolvation: 500 °C

Gas Flows:

Cone Gas: 50 L/hr

Desolvation Gas: 800 L/hr

LockSpray: Leucine-Enkephaline (556.2771 Da)

Scan Time: 0.1 sec

Interval: 10 sec

LCMS analysis 30 min method

LCMS analysis was carried out on a Waters Acquity UPLC system and a 30 min method with 5% to 60% B in 28.0 min. Mass spectra over a mass range from 120 m/z to 3000 m/z are acquired using positive-ion Electrospray Ionization (ESI). Deconvolution range from 10 – 150 kDa using Maximum Entropy (MaxEnt).

Column: Acquity UPLC BEH C4, 2.1 x 100mm Column, 1.7 µm
Column Temperature: 80°C
Eluents: A: water + 0.05% TFA; B: isopropanol + 0.05% TFA
Gradient: initial 5% B; from 5 % to 60 % B in 28.0 min; from 60 % B to 98 % B in 0.2 min; hold 1.1 min 98 % B
Flow rate: 0.5 mL/min
Injection Mode: Partial loop
MS Method: Time: 0 – 29.8 min

Mass Range: 120 – 3000 m/z
Ionization mode: ES+

Data: Continuum

Scan Time: 1 sec

QTof Tune Page: Source:

Capillary: 3.00 kV

Sampling Cone: 120 V

Source Offset: 30

Temperatures:

Source: 130 °C

Desolvation: 500 °C

Gas Flows:

Cone Gas: 50 L/hr

Desolvation Gas: 800 L/hr

<u>LockSpray</u>: Leucine-Enkephaline (556.2771 Da)

Scan Time: 0.1 sec

Interval: 10 sec

Peptide Mapping

Sample preparation was performed using iST sample preparation kit from Preomics and according to manufacturer's recommendation. Desalted tryptic peptides were analyzed on a nanoLC-MS instrument (Orbitrap-Exploris) with DDA method. Raw files were processed using the Mascot search engine (v. 2.6.0; Matrix Science, UK) using dansylcadaverine (+ 318.140199 Da) as variable modifications on glutamine and asparagine residues.

Preparation of amines

Dansylcadaverine (CAS 10121-91-2) was purchased from Sigma Aldrich.

Solubility values were measured following the protocols described by Tu et al.[40]
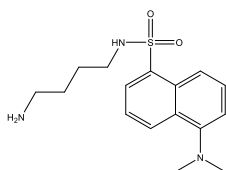
<u>A</u> : N-(4-aminobutyl)-5-(dimethylamino)naphthalene-1-sulfonamide was prepared according to described procedures.[41] HT-Eq pH 6.8 solubility [mM] : 0.498.
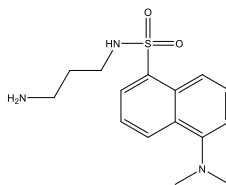
<u>B</u>: N-(3-aminopropyl)-5-(dimethylamino)naphthalene-1-sulfonamide was prepared according to described procedures.[42]
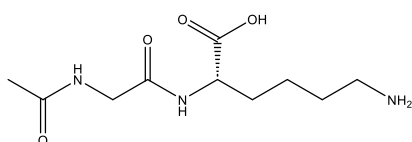HT-Eq pH 6.8 solubility [mM] : 0.561.

15
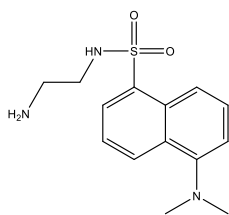
C: N-(2-aminoethyl)-5-(dimethylamino)naphthalene-1-sulfonamide was prepared according to described procedures.[43]
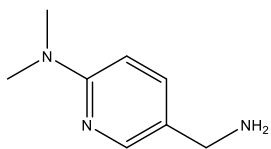
HT-Eq pH 6.8 solubility [mM] : 0.687.
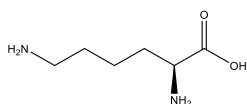
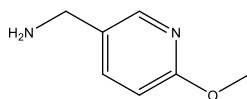D: CAS 657-27-2 was purchased from Sigma Aldrich.

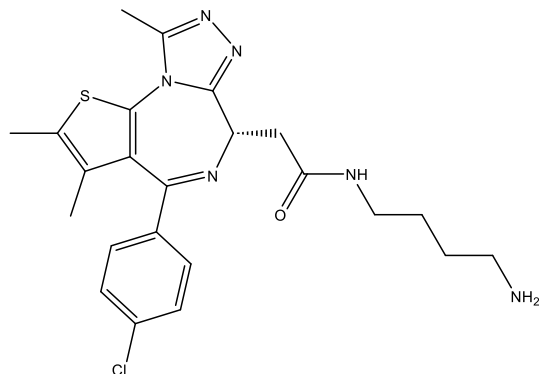E: CAS 10236-44-9 was purchased from ASW Medchem

F: CAS 19293-58-4 was purchased from Sigma Aldrich.

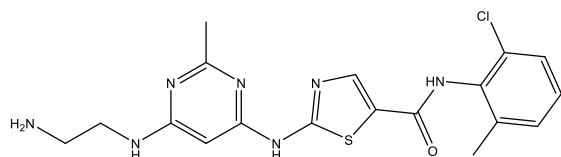HT-Eq pH 6.8 solubility [mM] : 0.459.

G: CAS 262295-96-5 was purchased from Sigma Aldrich.

HT-Eq pH 6.8 solubility [mM] : 0.227.¨

H: (S)-N-(4-aminobutyl)-2-(4-(4-chlorophenyl)-2,3,9-trimethyl-6H-thieno[3,2-f][1,2,4]triazolo[4,3-a][1,4]diazepin-6-yl)acetamide was prepared according to described procedures.[27]

HT-Eq pH 6.8 solubility [mM] > 0.75.

I: 2-((6-((2-aminoethyl)amino)-2-methylpyrimidin-4-yl)amino)-N-(2-chloro-6-methylphenyl)thiazole-5-carboxamide was prepared according to described procedures.[28]

HT-Eq pH 6.8 solubility [mM] = 0.175.
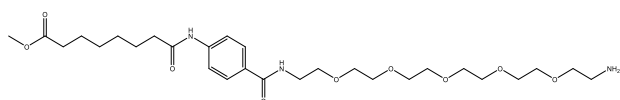
J: methyl 8-((4-((17-amino-3,6,9,12,15-pentaoxaheptadecyl)carbamoyl)phenyl)amino)-8-oxooctanoate preparation:

To a solution of 4-(8-methoxy-8-oxooctanamido)benzoic acid (320.0 mg, 1 eq, 1.041 mmol), O-(2-Aminoethyl)-O'-[2-(Boc-amino)ethyl]tetraethylene Glycol (396.1 mg, 1 eq, 1.041 mmol) and HATU (395.9 mg, 1 eq, 1.041 mmol) in DMF (3.000 mL) was added N-ethyl-N-isopropylpropan-2-amine (134.6 mg, 181 µL, 1 eq, 1.041 mmol) and the obtained mixture was stirred for 2 hours.

Ethyl acetate (100 mL) was added to the mixture and washed with 1M HCl, Sat. NaCO₃ and water and then dried over isolute phase separators. The volatile solvent mixture was evaporated

and the resulting product was treated with TFA (1.187 g, 802.1 µL, 10 eq, 10.41 mmol) in DCM (1:4 ratio) and stirred for 2 hours. Prep RP HPLC 0-100% (Water 0.2% formic acid/ Acetonitrile) gave the product methyl8-((4-((2-(2-(2-(2-aminoethoxy)ethoxy)ethoxy)ethyl)carbamoyl)phenyl)amino)-8-oxooctanoate (820.0 mg, 1.55 mmol, 79.6%, 100% Purity) as a white wax.

HT-Eq pH 6.8 solubility [mM] > 0.75.

^{1}H NMR (600 MHz, DMSO-*d6*) δ ppm 10.08 (s, 1H), 8.38 (t, *J* = 5.61 Hz, 1H), 7.79 (d, *J* = 8.64 Hz, 3H), 7.65 (d, *J* = 8.64 Hz, 3H), 3.57 (s, 4H), 3.46 - 3.54 (m, 27H), 3.32 - 3.43 (m, 12H), 3.02 - 3.10 (m, 3H), 2.63 (t, *J* = 5.83 Hz, 2H), 2.27 - 2.33 (m, 6H), 1.49 - 1.61 (m, 6H), 1.26 - 1.32 (m, 6H).

^{13}C NMR (151 MHz, DMSO-*d6*) δ ppm 173.3, 171.6, 165.7, 141.8, 128.6, 128.0, 118.1, 73.0, 69.8, 69.8, 69.7, 69.7, 69.6, 69.6, 69.5, 69.0, 51.2, 41.3, 40.1, 40.0, 39.1, 36.4, 33.2, 28.3, 28.2, 24.8, 24.3.

HRMS calculated for Chemical Formula $C_{28}H_{47}N_3O_9$ $[M+H]^+$ = 569.3312, Measured $[M+H]^+$ = 569.3386.

Lipofection studies

15000 HEPA1-6 cells per well (150 uL of media) were plated and the cells were recovered overnight. The lipoplex was prepared and incubated for 20 minutes. In the meantime, the compounds were diluted to 8 µM in DPBS and a serial dilution 1:2 from 100 nM to 0.39 nM was performed. A negative control containing only lipofectamine in PBS was set up. 50 uL of media was then removed from the plates and 50 µL of optimum containing the diluted siRNA was added, in order to have a final volume of 150 uL of media containing lipoplex. This was let in the hood 20 min before being incubated at 37°C for 24h. The cells were lysed and RT-PCR was performed.

ASSOCIATED CONTENT

LCMS data and NMR can be found in the Supporting Information.

AUTHOR INFORMATION

Corresponding Authors

* marie.flamme@novartis.com ; greg.mann@novartis.com

18

Author Contributions

MF, RG, DZ carried out the experiments. MF, AV performed the peptide mapping experiments and analysis. CB provided all amine compounds. MF, GM, DM, AB, RK designed the experiments. GM supervised the project. MF wrote the manuscript in consultation with all authors.

ACKNOWLEDGMENT

ABBREVIATIONS

ADC, antibody drug conjugate; BSA, Bovine serum albumin; bTG, *Bacillus subtilis* transglutaminase; DTT, dithiothreitol, E. Coli, *Escherichia Coli*; EGFR, epidermal growth factor receptor; IgG, immunogloblin G; mTG, *Streptomyces mobaraensis* transglutaminase; PEG, polyethlylene glycol; siRNA, small interfering ribonucleic acid; VHH, heavy chain variable.

REFERENCES

(1)   Kalia, J.; Raines, R. T. Advances in Bioconjugation. *Curr. Org. Chem.* **2010**, *14* (2), 138–147.

(2)   Hermanson, G. T. Chapter 1 - Introduction to Bioconjugation. In *Bioconjugate Techniques (Third Edition)*; Hermanson, G. T., Ed.; Academic Press: Boston, 2013; pp 1–125. https://doi.org/https://doi.org/10.1016/B978-0-12-382239-0.00001-7.

(3)   Healy, J. M.; Lewis, S. D.; Kurz, M.; Boomer, R. M.; Thompson, K. M.; Wilson, C.; McCauley, T. G. Pharmacokinetics and Biodistribution of Novel Aptamer Compositions. *Pharma. Res.* **2004**, *21* (12), 2234–2246. https://doi.org/10.1007/s11095-004-7676-4.

(4)   Lee, C. H.; Lee, S.-H.; Kim, J. H.; Noh, Y.-H.; Noh, G.-J.; Lee, S.-W. Pharmacokinetics of a Cholesterol-Conjugated Aptamer Against the Hepatitis C Virus (HCV) NS5B Protein. *Mol. Ther. - Nuc. Acids* **2015**, *4*, e254. https://doi.org/https://doi.org/10.1038/mtna.2015.30.

(5)   Alam, Md. R.; Ming, X.; Fisher, M.; Lackey, J. G.; Rajeev, K. G.; Manoharan, M.; Juliano, R. L. Multivalent Cyclic RGD Conjugates for Targeted Delivery of Small Interfering RNA. *Bioconj. Chem.* **2011**, *22* (8), 1673–1681. https://doi.org/10.1021/bc200235q.

(6)   Roberts, T. C.; Langer, R.; Wood, M. J. A. Advances in Oligonucleotide Drug Delivery. *Nat. Rev. Drug Discov.* **2020**, *19* (10), 673–694. https://doi.org/10.1038/s41573-020-0075-7.

(7)   Tsuchikama, K.; Anami, Y.; Ha, S. Y. Y.; Yamazaki, C. M. Exploring the next Generation of Antibody–Drug Conjugates. *Nat. Rev. Clin. Onc.* **2024**. https://doi.org/10.1038/s41571-023-00850-2.

(8)   Sornay, C.; Vaur, V.; Wagner, A.; Chaubet, G. An Overview of Chemo- and Site-Selectivity Aspects in the Chemical Conjugation of Proteins. *R. Soc. Open Sci.* **2022**, *9* (1). https://doi.org/10.1098/rsos.211563.

(9)   Anderson, G. W.; Zimmerman, J. E.; Callahan, F. M. N-Hydroxysuccinimide Esters in Peptide Synthesis. *J. Am. Chem. Soc.* **1964**, *85* (19), 1839–1842.

(10)   Debon, A.; Siirola, E.; Snajdrova, R. Enzymatic Bioconjugation: A Perspective from the Pharmaceutical Industry. *JACS Au* **2023**, *3* (5), 1267–1283. https://doi.org/10.1021/jacsau.2c00617.

(11)   Alexander, A. K.; Elshahawi, S. I. Promiscuous Enzymes for Residue-Specific Peptide and Protein Late-Stage Functionalization. *ChemBioChem* **2023**, *24* (17). https://doi.org/10.1002/cbic.202300372.

(12)   Duarte, L.; Matte, C. R.; Bizarro, C. V.; Ayub, M. A. Z. Transglutaminases: Part I—Origins, Sources, and Biotechnological Characteristics. *World J. Microbiol. Biotechnol* **2020**, *36* (1). https://doi.org/10.1007/s11274-019-2791-x.

(13)   Vasić, K.; Knez, Ž.; Leitgeb, M. Transglutaminase in Foods and Biotechnology. *Int. J. Mol. Sci.* **2023**, *24* (15). https://doi.org/10.3390/ijms241512402.

(14)   Deweid, L.; Avrutina, O.; Kolmar, H. Microbial Transglutaminase for Biotechnological and Biomedical Engineering. *Biol. Chem.* **2019**, *400* (3), 257–274. https://doi.org/doi:10.1515/hsz-2018-0335.

(15)   Strop, P.; Liu, S.-H.; Dorywalska, M.; Delaria, K.; Dushin, R. G.; Tran, T.-T.; Ho, W.-H.; Farias, S.; Casas, M. G.; Abdiche, Y.; Zhou, D.; Chandrasekaran, R.; Samain, C.; Loo, C.; Rossi, A.; Rickert, M.; Krimm, S.; Wong, T.; Chin, S. M.; Yu, J.; Dilley, J.; Chaparro-Riggers, J.; Filzen, G. F.; O'Donnell, C. J.; Wang, F.; Myers, J. S.; Pons, J.; Shelton, D. L.; Rajpal, A. Location Matters: Site of Conjugation Modulates Stability and Pharmacokinetics of Antibody Drug Conjugates. *Chem Biol* **2013**, *20* (2), 161–167. https://doi.org/https://doi.org/10.1016/j.chembiol.2013.01.010.

(16)   Zhang, D.; Zhu, Y.; Chen, J. Microbial Transglutaminase Production: Understanding the Mechanism. *Biotechnol. Genet. Eng. Rev.* **2009**, *26* (1), 205–222. https://doi.org/10.5661/bger-26-205.

(17)   Rickert, M.; Strop, P.; Lui, V.; Melton-Witt, J.; Farias, S. E.; Foletti, D.; Shelton, D.; Pons, J.; Rajpal, A. Production of Soluble and Active Microbial Transglutaminase in Escherichia Coli

for Site-Specific Antibody Drug Conjugation. *Prot. Sci.* **2016**, *25* (2), 442–455. https://doi.org/https://doi.org/10.1002/pro.2833.

(18) Oteng-Pabi, S. K.; Clouthier, C. M.; Keillor, J. W. Design of a Glutamine Substrate Tag Enabling Protein Labelling Mediated by Bacillus Subtilis Transglutaminase. *PLoS One* **2018**, *13* (5). https://doi.org/10.1371/journal.pone.0197956.

(19) Jeger, S.; Zimmermann, K.; Blanc, A.; Grünberg, J.; Honer, M.; Hunziker, P.; Struthers, H.; Schibli, R. Site-Specific and Stoichiometric Modification of Antibodies by Bacterial Transglutaminase. *Angew. Chem. Int. Ed.* **2010**, *49* (51), 9995–9997. https://doi.org/10.1002/anie.201004243.

(20) Fontana, A.; Spolaore, B.; Mero, A.; Veronese, F. M. Site-Specific Modification and PEGylation of Pharmaceutical Proteins Mediated by Transglutaminase. *Adv. Drug Deliv. Rev.* **2008**, *60* (1), 13–28. https://doi.org/10.1016/j.addr.2007.06.015.

(21) Kieliszek, M.; Misiewicz, A. Microbial Transglutaminase and Its Application in the Food Industry. A Review. *Folia Microbiol.* **2014**, *59* (3), 241–250. https://doi.org/10.1007/s12223-013-0287-x.

(22) Kükenshöner, T.; Schmit, N. E.; Bouda, E.; Sha, F.; Pojer, F.; Koide, A.; Seeliger, M.; Koide, S.; Hantschel, O. Selective Targeting of SH2 Domain–Phosphotyrosine Interactions of Src Family Tyrosine Kinases with Monobodies. *J. Mol. Biol.* **2017**, *429* (9), 1364–1380. https://doi.org/10.1016/j.jmb.2017.03.023.

(23) Kim, R. K.; Yoon, C. H.; Hyun, K. H.; Lee, H.; An, S.; Park, M. J.; Kim, M. J.; Lee, S. J. Role of Lymphocyte-Specific Protein Tyrosine Kinase (LCK) in the Expansion of Glioma-Initiating Cells by Fractionated Radiation. *Biochem. Biophys. Res. Comm.* **2010**, *402* (4), 631–636. https://doi.org/10.1016/j.bbrc.2010.10.072.

(24) Bommhardt, U.; Schraven, B.; Simeoni, L. Beyond TCR Signaling: Emerging Functions of Lck in Cancer and Immunotherapy. *Int. J. Mol. Sci.* **2019**, *20* (14), 3500–3518. https://doi.org/10.3390/ijms20143500.

(25) Liu, Y.; Huang, L.; Zheng, D.; Fu, Y.; Shan, M.; Li, Y.; Xu, Z.; Jia, L.; Wang, W.; Lu, F. Characterization of Transglutaminase from: Bacillus Subtilis and Its Cross-Linking Function with a Bovine Serum Albumin Model. *Food Funct.* **2018**, *9* (11), 5560–5568. https://doi.org/10.1039/c8fo01503a.

(26) Veenstra, T. D.; Van, Q. N.; Fox, S. D.; Issaq, H. J. Chapter 16 - Protein and Metabolite Identification. In *Proteomic and Metabolomic Approaches to Biomarker Discovery*; Issaq, H. J., Veenstra, T. D., Eds.; Academic Press: Boston, 2013; pp 245–258. https://doi.org/https://doi.org/10.1016/B978-0-12-394446-7.00016-9.

(27) Xue, G.; Wang, K.; Zhou, D.; Zhong, H.; Pan, Z. Light-Induced Protein Degradation with Photocaged PROTACs. *J. Am. Chem. Soc.* **2019**, *141* (46), 18370–18374. https://doi.org/10.1021/jacs.9b06422.

(28) Shi, H.; Zhang, C.-J.; Chen, G. Y. J.; Yao, S. Q. Cell-Based Proteome Profiling of Potential Dasatinib Targets by Use of Affinity-Based Probes. *J. Am. Chem. Soc.* **2012**, *134* (6), 3001–3014. https://doi.org/10.1021/ja208518u.

(29) Khongorzul, P.; Ling, C. J.; Khan, F. U.; Ihsan, A. U.; Zhang, J. Antibody–Drug Conjugates: A Comprehensive Review. *Mol. Cancer Res.* **2020**, *18* (1), 3–19. https://doi.org/10.1158/1541-7786.MCR-19-0582.

(30) Tai, W. Current Aspects of SiRNA Bioconjugate for In Vitro and In Vivo Delivery. *Molecules* **2019**, *24* (12), 2211.

(31) Huggins, I. J.; Medina, C. A.; Springer, A. D.; Van den Berg, A.; Jadhav, S.; Cui, X.; Dowdy, S. F. Site Selective Antibody-Oligonucleotide Conjugation via Microbial Transglutaminase. *Molecules* **2019**, *24* (18), 3287.

(32) Zhou, Q. Site-Specific Antibody Conjugation with Payloads beyond Cytotoxins. *Molecules* **2023**, *28* (3), 917.

(33) Konč, J.; Brown, L.; Whiten, D. R.; Zuo, Y.; Ravn, P.; Klenerman, D.; Bernardes, G. J. L. A Platform for Site-Specific DNA-Antibody Bioconjugation by Using Benzoylacrylic-Labelled Oligonucleotides. *Angew. Chem. Int. Ed.* **2021**, *60* (49), 25905–25913. https://doi.org/https://doi.org/10.1002/anie.202109713.

(34) Shao, J.; Wang, L.; Zhong, C.; Qi, R.; Li, Y. AHSA1 Regulates Proliferation, Apoptosis, Migration, and Invasion of Osteosarcoma. *Biomed. Pharmacother.* **2016**, *77*, 45–51. https://doi.org/https://doi.org/10.1016/j.biopha.2015.11.008.

(35) Copolovici, D. M.; Langel, K.; Eriste, E.; Langel, Ü. Cell-Penetrating Peptides: Design, Synthesis, and Applications. *ACS Nano* **2014**, *8* (3), 1972–1994. https://doi.org/10.1021/nn4057269.

(36) Gonzalez-Sapienza, G.; Rossotti, M. A.; Tabares-da Rosa, S. Single-Domain Antibodies As Versatile Affinity Reagents for Analytical and Diagnostic Applications. *Front Immunol.* **2017**, *8*.

(37) Bever, C. S.; Dong, J.-X.; Vasylieva, N.; Barnych, B.; Cui, Y.; Xu, Z.-L.; Hammock, B. D.; Gee, S. J. VHH Antibodies: Emerging Reagents for the Analysis of Environmental Chemicals. *Anal. Bioanal. Chem.* **2016**, *408* (22), 5985–6002. https://doi.org/10.1007/s00216-016-9585-x.

(38) Sabbah, D.; Hajjo, R.; Sweidan, K. Review on Epidermal Growth Factor Receptor (EGFR) Structure, Signaling Pathways, Interactions, and Recent Updates of EGFR Inhibitors. *Curr. Top. Med. Chem.* **2020**, *20* (10), 815–834.

(39) Candelaria, P. V.; Leoh, S. L.; Penichet, M. L.; Daniels-Wells, T. R. Antibodies Targeting the Transferrin Receptor 1 (TfR1) as Direct Anti-Cancer Agents. *Front. Immunol.* **2021**, *12*, 607692.

(40) Tu, H.-F.; Jeandin, A.; Bon, C.; Brocklehurst, C.; Lima, F.; Suero, M. G. Late-Stage Aryl C−H Bond Cyclopropenylation with Cyclopropenium Cations. *Angew. Chem. Int. Ed.* **2023**, *62* (36), e202308379. https://doi.org/https://doi.org/10.1002/anie.202308379.

(41) Akbar, A.; McNeil, N. M. R.; Albert, M. R.; Ta, V.; Adhikary, G.; Bourgeois, K.; Eckert, R. L.; Keillor, J. W. Structure-Activity Relationships of Potent, Targeted Covalent Inhibitors That Abolish Both the Transamidation and GTP Binding Activities of Human Tissue Transglutaminase. *J. Med. Chem.* **2017**, *60* (18), 7910–7927. https://doi.org/10.1021/acs.jmedchem.7b01070.

(42) Sikkema, F. D.; Comellas-Aragonès, M.; Fokkink, R. G.; Verduin, B. J. M.; Cornelissen, J. J. L. M.; Nolte, R. J. M. Monodisperse Polymer-Virus Hybrid Nanoparticles. *Org. Biomol. Chem.* **2007**, *5* (1), 54–57. https://doi.org/10.1039/b613890j.

(43) Kurono, M.; Isobe, M. Synthesis and Physical Nature of Fluorescent Photoaffinity Probe for the Bioorganic Studies on Tautomycin, a Protein Phosphatase Type 1 Selective Inhibitor. *Chem. Lett.* **2004**, *33* (4), 452–453. https://doi.org/10.1246/cl.2004.452.

24